80895_Auto_Edited-check.docx

WORD COUNT	8937	TIME SUBMITTED	25-DEC-2022 09:49PM
		PAPER ID	94357120

Bowel inflammatory presentations on computed tomography in adult patients with severe aplastic anemia during flared inflammatory episodes

Zhao XC *et al*. Abdominal CT imaging in SAA

Xi-Chen Zhao, Cheng-Jiang Xue, Hui Song, Bin-Han Gao, Fu-Shen Han, Shu-Xin Xiao

Abstract

BACKGROUND

Patients with severe aplastic anemia (SAA) frequently present with inflammatory episodes, and during flared inflammatory episodes, hematopoietic function is further exacerbated. The gastrointestinal tract is the most common site for infectious and inflammatory diseases, and its structural and functional features confer on it the most potent capacity to affect hematopoietic and immune functions. Computed tomography (CT) is a readily accessible approach to provide highly useful information in detecting morphological changes and guiding further work-ups.

AIM

To explore CT imaging presentations of gut inflammatory damage in adult SAA patients during inflammatory episodes.

METHODS

We retrospectively evaluated the abdominal CT imaging presentations of 17 hospitalized adult patients with SAA in search of the inflammatory niche when they presented with systemic inflammatory stress and exacerbated hematopoietic function. In this descriptive manuscript, the characteristic images that suggested the presence of gastrointestinal inflammatory damage and related imaging presentations of individual patients were enumerated, analyzed and described.

RESULTS

All eligible patients with SAA had CT imaging abnormalities that suggested the presence of an impaired intestinal barrier and increased epithelial permeability. The inflammatory damages were concurrently present in the small intestine, the ileocecal region and the large intestines. Some readily identified imaging signs, such as bowel wall thickening with mural stratification ("water holo sign", "fat holo sign", intramural gas and subserosal pneumatosis) and mesenteric fat proliferation (fat stranding and "creeping fat sign"), fibrotic bowel wall thickening, "balloon sign", rugged colonic configuration, heterogeneity in the bowel wall texture, and adhered and clustered small bowel loop (including various patterns of "abdominal cocoon"), occurred at a high incidence, which suggested that the damaged gastrointestinal tract is a common inflammatory niche responsible for the systemic inflammatory stresses and the exacerbated hematopoietic failure in patients with SAA. Particularly, the "fat holo sign" was present in 7 patients, a rugged colonic configuration was present in 10 patients, the adhesive bowel loop was present in 15 patients, and extraintestinal manifestations suggestive of tuberculosis infections were present in 5 patients. According to the imaging features, a suggestive diagnosis of Crohn's disease was made in 5 patients, ulcerative colitis in 1 patient, chronic periappendiceal abscess in 1 patient, and tuberculosis infection in 5 patients. Other patients were diagnosed with chronic enteroclolitis with acutely aggravated inflammatory damage.

CONCLUSION

Patients with SAA had CT imaging patterns that suggested the presence of active chronic inflammatory conditions and aggravated inflammatory damage during flared inflammatory episodes.

Key Words: Aplastic anemia; Computed tomography; Bowel inflammatory damage; Fat holo sign; Balloon sign; Abdominal cocoon

Zhao XC, Xue CJ, Song H, Gao BH, Han FS, Xiao SX. Bowel inflammatory presentations on computed tomography in adult patients with severe aplastic anemia during flared inflammatory episodes. *World J Clin Cases* 2022; In press

Core Tip: Patients with severe aplastic anemia frequently present with inflammatory episodes. The gastrointestinal tract is the most common site for infectious and inflammatory diseases, and its structural and functional features confer on it the most potent capacity to affect hematopoietic and immune functions. We retrospectively reviewed the bowel morphological changes on computed tomography in seventeen patients with severe aplastic anemia during fared inflammatory episodes. All patients demonstrated imaging abnormalities that suggested the presence of active chronic inflammatory conditions and aggravated inflammatory damage in the gastrointestinal tract. These inflammatory conditions likely contributed to their systemic inflammatory stresses and exacerbated hematopoietic failure.

INTRODUCTION

Aplastic anemia (AA) is the paradigm of hematopioetic failure resulting from the immune-mediated destruction of hematopoietic progenitor cells, leading to heavily suppressed blood cell productivity and peripheral cytopenia. In patients with severe AA (SAA), fulminant infections, frequently in the absence of localized symptoms and signs, and refractory to broad-spectrum antibiotics, are the most common complications and the main causes of death. Infections in SAA are usually attributed to severely impaired granulopoiesis, and it frequently has a poor response to recombinant human granulocyte colony-stimulating factor (rhG-CSF) treatment[1-3]. However, successful treatment of the underlying infections can significantly improve the hematological profile and even achieve a complete hematological remission in some patients, providing strong evidence that aggravated inflammatory reactions are responsible, at least in a fraction of patients, for the exacerbated hematopoietic suppression[4-6]. Very recently, initiation and perpetuation of AA pathogenesis has been found to be

associated with gut inflammatory disorders (GIDs)[7,8]. However, the role of GIDs in AA pathogenesis is overlooked likely due to the high prevalence and good tolerance of GIDs and the low incidence of AA.

The gastrointestinal tract hosts the most enriched and complex microbial community in the human body. Not only pathogenic microbes but also dysbiotic commensal bacteria and various chemical components can compromise the intestinal barrier[9,10]. In the setting of impaired intestinal barrier structure and function, antigens from commensal microbes and undigested food as a source of continuous antigen supply can translocate to the lamina propria, blood, and remote organs and come into intimate contact with host immune cells, thereby initiating and perpetuating autoimmunity[11,12] and amplifying aberrant immune responses[13]. The gastrointestinal tract also hosts the most enriched lymphoid tissues and hence can provide sufficient activated immune cells to sustain exaggerated immune responses. Because the body is constantly confronted with various harmful environmental factors, the gastrointestinal tract is the most common site for infectious and inflammatory diseases[9,10].

Active GIDs, whether as a consequence or as an incentive factor in the process of gut dysbiosis and epithelial damage, can lead to morphological manifestations that can be detected by various imaging modalities. The imaging presentations are usually nonspecific, and arriving at an etiopathological diagnosis usually necessitates the comprehensive analysis of data from clinical, endoscopic, pathological and laboratory investigations, and is frequently dependent on the results of specific laboratory tests and the responses to specific treatments. However, computed tomography (CT) is a readily accessible approach able to provide highly useful information not only in detecting the distribution, extent, degree, and patterns of the gastrointestinal lesions and the adjacent inflammatory changes that prompt a radiological diagnosis but also in guiding further work-ups for pathognomonic diagnosis, identifying complications, evaluating treatment responses and monitoring disease activities in the subsequent follow-ups[14-16]. In this study, we explored the CT imaging manifestations of the gastrointestinal tract in adult patients with SAA during flared inflammatory episodes

and showed that all patients had imaging abnormalities suggesting the presence of active chronic gut inflammatory conditions and acutely aggravated inflammatory damages.

MATERIALS AND METHODS

Participants

In this retrospective study, we reviewed the abdominal CT images in 17 hospitalized adult SAA patients who were treated at our center from October 2019 to March 2022, including 8 males and 9 females, with a median age of 55 years (ranging from 34 to 78 years). They were hospitalized due to rapidly exacerbated cytopenia, aggravated fatigue, varying degrees of febrile episodes and elevated inflammatory indices, indicating the presence of systemic inflammatory responses[1-3]. Each patient was definitively diagnosed with SAA for more than 2 years, and the SAA progressed from non-SAA (NSAA) after the patients experienced various accelerating episodes. In addition to supportive care, they were routinely treated with cyclosporine (3-4 mg/kg·d), stanozolol (6-8 mg/d) and eltrombopag (50 mg/d) in the SAA stage, in the absence of any therapeutic responses. In the patients with very SAA (VSAA), recombinant human granulocyte colony-stimulating factor (rhG-CSF, 100-200 μg/d) was added, without an evident increase in granulocytes. Patients who had diseases of portal hypertension, hepatic disease, pancreatic disease, cardiopulmonary disease, heart failure, severe hypoalbuminemia and ischemic enteropathy were excluded, because these diseases can cause stratified bowel wall thickening by blood congestion in the gastrointestinal tract, which may confound the imaging presentations of inflammatory lesions[16-18]. Abdominal CT was performed to search for the inflammatory niche before antibiotic and other treatments.

The modified Camitta criteria were used to assess severity of AA[3]: The diagnostic criteria for SAA were absolute neutrophil count (ANC) < 0.5 × 10^9/L, platelets (Plts) < 20 × 10^9/L, and absolute reticulocyte count (Ret) < 20 × 10^9/L. The diagnostic criteria

for VSAA were ANC < 0.2 × 10^9/L in addition to the above hematological presentations.

Study procedure

CT imaging modalities: Conventional CT was performed for all patients in the search of the inflammatory niche during flared inflammatory episodes. If the conventional CT was sufficient to determine the radiological changes, contrast-enhanced CT was waived in order to reduce the radiation exposure. If the conventional CT was unable to determine the imaging abnormalities due to the difficulty in the discrimination of a massive lesion from contents in the intestinal lumen or due to the suspicion of a massive lesion being malignant, contrast-enhanced CT was performed. Meanwhile, endoscopic examination of the large intestine and ileocecal region was performed. Contrast-enhanced CT was performed in 1 patient in this study. Multiplanar reconstruction was performed for the assessment and expression of the radiological manifestations.

CT image reviewing process: Each patient's CT images were reviewed, and the imaging abnormalities were collected independently by each of the six authors: Xi-Chen Zhao, Cheng-Jiang Xue, Hui Song, Bin-Han Gao, Fu-Sen Han, and Shu-Xin Xiao. After several rounds of extensive consultation, the imaging abnormalities suggesting the presence of GIDs were decided by the first and corresponding author. In patients with evident chest CT presentations that likely had pathogenic relationships with the bowel inflammatory damages; those chest CT abnormalities were also enumerated and described.

Radiological manifestations suggesting the gut involvement of inflammatory disorders: After careful assessment of the radiographs and after extensive consultations within our research group with reference to the patients' symptoms and signs, the

following imaging presentations were considered to have abnormalities suggestive of the presence of GIDs:

First, the criteria for the diagnosis of bowel wall thickening met one of the following criteria[17-21]: (1) Bowel wall thickness greater than 3 mm in adequately distended intestinal segments; (2) bowel wall thickness greater than 4 mm in underdistended intestinal segments; (3) cross-sectional diameter greater than 6 mm in collapsed small intestines; and (4) cross-sectional diameter greater than 5 mm in collapsed large intestines.

The bowel wall thickening may be focal or segmental, symmetrical or asymmetrical, concentric or eccentric, homogeneous or heterogeneous. The following signs were helpful in the identification of the location and extent of the diseased bowel segments: (1) Mesenteric inflammatory changes indicative of transmural inflammation: "fat stranding"[22,23], "creeping fat sign"[24-26] and "comb sign"[27,28]; (2) mural stratification indicative of edematous bowel wall (water holo sign) and submucosal fat deposition (fat holo sign)[17-21]; (3) intramural gas and/or subserosal pneumatosis indicative of aerogenous bacterial proliferation in the bowel wall[14-16]; (4) gas-liquid levels in the intestinal lumen indicative of intestinal dynamical abnormalities; (5) heterogeneity in the bowel wall texture especially with segmentally gas-filled and segmentally liquid-filled intestinal lumen; (6) inflamed diverticulitis; (7) epiplioic appendagitis; (8)"empty colon sign" or narrowed bowel lumen[15,16]; (9) adhesive bowel loop, especially with mesenteric inflammatory changes and/or adjacent peritoneal fibrotic thickening ("abdominal cocoon")[29-32]; and (10) rugged colonic configuration, especially with mesenteric inflammatory changes and/or adjacent peritoneal fibrotic thickening.

Second, the "balloon sign" refers to a segment of a paper-thin bowel wall (a highly dilated and thinned bowel segment filled with gas) wrapped by a large cluster of circumferentially distributed hypervascular mesenteric fat stranding[33-36]. The hypervascular mesenteric fat deposition suggests the presence of active chronic transmural inflammatory damage in the diseased intestinal segments[22-26].

Third, peritoneal involvement: Including peritoneal thickening, ascites particularly loculated ascites and peritoneal nodularity.

In the evaluation of bowel inflammatory damage, particular attention was given to imaging abnormalities in the large intestines and ileocecal region, since in these sites, the lymphoid tissues are the most enriched and the microbial community is the most abundant; therefore, inflammatory damage and compromised epithelial integrity in these intestinal segments has the most potent capability to supply sufficient intestine-derived antigens and to activate sufficient immune cells and hence has the most potent capability to affect hematopoietic and immune functions[9,10].

This study was approved by the Institutional Review Board of The Central Hospital of Qingdao West Coast New Area and followed the Declaration of Helsinki (No. 2022-10-08). The requirement for written informed consent was waived by the Review Board since this was a retrospective study, and no information about patient identification was revealed in the manuscript.

Statistical analysis

Categorical data are presented as numbers with percentages, and continuous data are presented as medians with interquartile ranges.

RESULTS

General characteristics of patients

General information, severity of AA, disease duration, complete blood cell count (CBC) results when abdominal CT was performed, major gastrointestinal presentations and suggested radiological diagnosis are listed in Table 1. Seventeen patients (8 men and 9 women) with a median age of 55 years, ranging from 34 to 78 years were enrolled. The total AA duration ranged from 8 to 23 years, with a median duration of 13 years, and the total SAA duration ranged from 2 years to 9 years, with a median duration of 5 years. Among all patients, 5 had VSAA. Abdominal tenderness was present in all patients, but abdominal pain was present in only 8 patients, in accordance with the

good tolerance of GIDs. Abnormalities in the frequency and property of the feces were present in 11 patients.

CT imaging abnormalities reflecting gut involvement of inflammatory conditions

Characteristic images are enumerated, analyzed and described in the Discussion section. All patients recruited in this study presented with evident imaging abnormalities that suggested the presence of inflammatory damages in the gastrointestinal tract. Noticeably, inflammatory involvement of the large intestine and the ileocecal region was present in all patients. Inflammatory lesions were also present in the small intestine in all patients, suggesting that the inflammatory pathogenesis was most likely initiated at the proximal gastrointestinal tract. According to the imaging features, a suggestive diagnosis of Crohn's disease was made in 5 patients, ulcerative colitis in 1 patient, chronic periappendiceal abscess in 1 patient, and tuberculosis infection in 5 patients. Other patients were diagnosed with chronic enteroclolitis with acutely aggravated inflammatory damage. The suggested radiological diagnosis is listed in Table 1.

DISCUSSION

The severity of cellular immune-mediated hematopoietic suppression in patients with AA commonly fluctuates in parallel with the waxing and waning of physical and mental stresses, and these stresses are obviously driven by active chronic inflammatory conditions and their recurrently aggravated episodes. In flared inflammatory episodes, blood cell production is heavily suppressed, and cytopenia worsens. With effective treatment of the inflammatory episodes, blood cell productivity can be significantly improved. Along with the increased frequency of and decreased intervals between these inflammatory episodes, patients eventually enter into an advanced stage, in which immune-mediated hematological damage is exacerbated and the sensitivity to previous effective treatments is lost[1,2,37,38].

This is not surprising because the blood cells themselves are immune cells, and their production is regulated largely in response to a variety of microbial attacks. When confronting an acute and limited infection, host hematopoiesis skews its proliferation and differentiation toward the production of innate immune cells to fight against the invading microbes at the expense of reduced self-renewal capacity[39,40]. After the infected pathogens are cleared out, the activated host immune system quickly returns to the homeostatic state, and the skewed blood cell production ends. However, in the setting of active chronic inflammatory conditions or overwhelming infections, host hematopoiesis can be heavily suppressed and exhausted due to prolonged and exaggerated immune responses and the subsequently overproduced proinflammatory mediators[41-43], resulting in heavily decreased marrow cellularity and increased peripheral cytopenia in genetically susceptible subjects, which are the characteristic morphological and immunological changes seen in AA[1-3]. The sustenance of an active inflammatory condition in which the degree and duration of immune responses are sufficient to induce severe aplastic cytopenia critically necessitates sufficient activated immune cells and a continuous antigen supply.

The gastrointestinal tract provides the largest interface bridging the host neuro-endocrine-immune system with environmental factors and is constantly confronted with a variety of environmental challenges. The gastrointestinal tract also hosts the body's most abundant gut-associated lymphoid tissues) and microbial community[9,10]. These structural and functional characteristics make the gastrointestinal tract the most vulnerable site for pathogen invasion and chemical injuries and the most common source of a continuous antigen supply. Therefore, the gastrointestinal tract becomes the most important site for pathological interactions between host immune cells and pathogenic antigens.

The gastrointestinal tract is the most common site for chronic and active inflammatory niches not only due to various pathogenic microbial attacks and chemical injuries but also due to dysbiotic commensal microbes and autoimmunity. Such abundant lymphoid tissues and microbial communities confer on the gastrointestinal

tract the ability to provide sufficient activated immune cells and a continuous antigen supply and thereby have the most potent capacity to continuously release excessive proinflammatory cytokines.

Under chronic and active inflammatory conditions, upregulated human leukocyte antigen and pattern recognition receptors on hematopoietic progenitors enhance their responsiveness to pathogenic stimulation[44-46], and upregulated Fas molecules accelerate their apoptotic cell death[45], eventually resulting in the exhaustion of hematopoietic progenitor cells. The severity of GIDs is largely affected by changes in a variety of environmental factors, such as food supplements[47-49], antibiotic abuse[50,51], mental stresses[52,53] and pathogen invasion, leading to the fluctuant property of GIDs, in accordance with the fluctuant property of AA.

AA has been reported to be associated with gut inflammatory diseases, including inflammatory bowel disease, celiac disease and neutropenic enterocolitis[8]. In our previously reported case, intermittent treatments with a gut-cleansing preparation achieved reproducible hematological remissions, providing direct evidence for the role of GIDs in the initiation and perpetuation of AA pathophysiology[4]. Merely gluten-free diets[5] or resection of diseased intestinal segments[6] can achieve excellent hematological improvement, providing convincing evidence that GIDs play an indispensable role in the sustenance of AA pathophysiology.

In this pathogenic process, impaired intestinal integrity and increased epithelial permeability play pivotal roles[11,12]. These GID-associated morphological changes could be detected by various imaging modalities. Abdominal CT is a readily accessible and highly efficient imaging modality for detecting morphological changes in the gastrointestinal tract[14-16,19,20]. In this study, we explored the abdominal imaging presentations in patients with SAA in search of the inflammatory niche when the patients presented with systemic inflammatory stresses. We selected patients with SAA experiencing flared episodes because during this stage, morphological changes due to the gut inflammation are probably more serious and hence more easily ientified by radiological examination.

In the evaluation of abdominal CT imaging abnormalities, particular attention has been given to inflammatory abnormalities in the ileocecal region and the colonic segments because they host the most enriched microbial community and lymphoid tissues[9,10,19]; therefore, inflammatory diseases and compromised intestinal barriers in these bowel segments have the most potent capacity to provide sufficient intestine-derived antigens and activated immune cells to affect hematopoietic and immune functions irrespective of whether they are primary damage or secondary to dysbiotic gut microbiota. As demonstrated by this study, all patients with SAA during flared inflammatory episodes had evident morphological abnormalities that could reflect the presence of a severely damaged intestinal structure and function in the ileocecal region and the colonic segments. All patients also presented with inflammatory damages in the proximal small intestine, suggesting that inflammatory damages in the upper gastrointestinal tract led to the inflammatory damages in the downstream intestinal segments, probably by altering the gut microbial composition[54-56]. In the following sections, we described the characteristic CT imaging findings in each patient in the category of readily identified morphological presentations.

All patients demonstrated CT imaging abnormalities that suggested the presence of gut inflammatory damage in the large intestine. Colonic wall thickening with mural stratification, intramual gas and paracolonic fat stranding is the common presentation of colonic involvement of inflammatory damage. A stratified bowel wall can be caused by submucosal fat deposition (fat holo sign) or submucosal edematous tissues (water holo sign)[17-19]. The water holo sign was present in 8 patients [cases 1 (Figure 14), 2 (Figure 12), 3 (Figure 3), 6 (Figure 4), 9 (Figure 5), 12 (Figure 15), 14 (Figure 1) and 15 (Figure 10)], commonly accompanying intramural gas and subserosal peumatosis, which indicated the presence of aerogenous bacterial proliferation in the colonic wall irrespective of primary infection or infection secondary to dysbiotic microbiota, acute episodes or chronic damage[22,23]. The fat holo sign which suggested the existence of active chronic gut inflammation was detected in 7 patients [cases 1 (Figure 14), 4 (Figure 1), 9 (Figure 5), 11 (Figure 11), 13 (Figure 2), 16 (Figure 17) and 17 (Figure 13)]. In these 7

patients, the fat holo sign was located in the ileocecal region and proximal ascending colon.

The "balloon sign" is characterized by circumferentially distributed clustering of hypervascular mesenteric fat proliferation wrapping a short segment of highly distended paper-thin bowel wall[33,34]. The "balloon sign"can also be seen in a large subserosal pneumatosis[35,36]. The circumferentially distributed clustering of hypervascular fat proliferation suggests the presence of an active chronic inflammatory condition in diseased intestinal segments. The balloon sign was present in 7 patients. The paper-thin bowel wall can be the wall of either the small or large intestine. In case 3 (Figure 3), the paper-thin bowel wall was present in the proximal ileum. In case 14 (Figure 8), the paper-thin bowel wall was present in the ascending colon. In case 17 (Figure 13), the paper-thin bowel wall was present in the hepatic flexure. In cases 6 (Figure 4), 7 (Figure 15), 8 (Figure 16), and 9 (Figure 5), the paper-thin bowel wall was present in the sigmoid colon.

The "empty colon sign" refers to a colonic segment in which any contents are absent, usually in a segmentally wall-thickened colon or following a focally wall-thickened colon. Malignant masses are the most common cause. However, inflammatory diseases can also cause empty colon signs, especially in segmental thickening of the colonic wall with edematous submucosal tissues and prominent mesenteric fat stranding[15-18]. In this study, 6 patients presented with an empty colon sign. In case 9 (Figure 5), the collapsed transverse and descending colon followed the segmentally wall-thickened colon in the hepatic flexure, and endoscopic examination later demonstrated a polypoid lesion in the diseased colonic segment. In case 1 (Figure 14), the empty colon sign was exhibited as a long segment of the thickened, stratified and emptied ascending and proximal transverse colon. In case 13 (Figure 2), the empty colon sign was exhibited a thickened, stratified and emptied colonic segment in the hepatic flexure, followed by the collapsed proximal transverse colon. In cases 3 (Figure 3), 4 (Figure 1) and 15 (Figure 10), the empty colon sign was exhibited a segmentally thickened, stratified and emptied colon in the hepatic flexure.

The "creeping fat sign" represents an imaging presentation in which proliferated fat deposition leads to the widening of the bowel loop[24]. The appearance of the creeping fat sign signifies the presence of chronic transmural inflammation in diseased intestinal segments[16,18,24,25]. In case 10 (Figure 6), the silt-like fat deposition led to the widening of the small bowel loop. In the ileal segment, the wall was thickened, and the lumen was dilated. In case 8 (Figure 16), similar imaging features were shared with those in case 10. However, case 8 presented concomitantly with infectious lesions in the pleura, indicative of the reactivation of old tuberculosis.

Diffused bowel inflammatory damage in Crohn's disease predominantly affects the small intestine, and the ileocecal valve and large intestine are commonly involved. The "creeping fat sign" is the characteristic imaging presentation in the diagnosis of Crohn's disease[24,25]. In case 10, the "creeping fat" manifested as silt-like fat deposition. However, most patients manifested perienteric hypervascular fat proliferation wrapping the fibrotically thickened wall and dilated lumen of the ileal segment. Four patients (cases 8, 9, 12, and 14) were found to have this radiological feature. In case 8 (Figure 16), this form of creeping fat was present in the distal jejunum, whereas in the other 3 patients [case 9 (Figure 6), 12 (Figure 7) and 14 (Figure 8)], creeping fat was present in the ileum. They also presented with other forms of inflammatory changes in the small and large intestines.

While the diffuse bowel inflammatory lesions of Crohn's disease predominate in the small intestine, the bowel inflammatory lesions of ulcerative colitis predominate in the colon. Fibrotic thickening of the colonic wall is a common imaging presentation, usually with striking paracolonic hypervascular mesenteric fat proliferation, indicating chronic lesions in nature, different from those of acute colonic infectious diseases[15-19]. The ileocecal region and small intestine are commonly involved in various forms of inflammatory damages. These imaging features were present in case 5 (Figure 9). In addition to fibrotic thickening of the colonic wall and the dilated colonic lumen, peritoneal thickening and loculated ascites in the iliac fossa and pelvic cavity indicated peritoneal involvement of inflammatory lesions. The hypertrophic lesion in the pluera

with pleural effusion suggested the presence of tuberculosis infection. These imaging features indicated that tuberculosis infection likely initiated the gut inflammatory condition in this case.

Marked irregular mucosal contour and fibrotically thickened mucosal folds of the large intestine, commonly with colonic wall thickening and subserosal pneumatosis, makes the colonic configuration rugged. This rugged colonic configuration especially with peritoneal thickening could suggest an existence of active and chronic inflammatory conditions in diseased colonic segment. It commonly occurs in the ascending colon and coexists omental involvement and pronounced paracolonic fat stranding. This easily recognized imaging presentation is highly useful in the identification of colonic inflammatory damages which is distinguishable from edematous thickening of the colonic wall with dispropositionately less severe paracolonic fat stranding in acute enterocolotis[14-18]. In patients presented with this imaging presentation, inflammatory lesions also involved other colonic segments, the ileocecal region and small intestine. The rugged configuration of the descending colon presented in 10 patients [case1 (Figure 14), 2 (Figure 12), 3 (Figure 3), 4 (Figure 1), 8 (Figure 16), 9 (Figure 5), 11 (Figure 11), 15 (Figure 10), 16 (Figure 17), and 17 (Figure 13)], suggesting that it is common imaging presentations in patients with SAA, in accordance with the high prevalence of inflammatory and infectious diseases in the ileocecal region and the proximal ascending colon.

The “adhesive bowel loop” refers to a segment of small bowel that has adhered and clustered. Various bowel wall abnormalities could be present in the adhered and clustered small bowel segments. Heterogeneity in the bowel wall texture was commonly striking in the adhered small bowel segment. The lumen could be either gas-filled or liquid-filled and frequently alternated. Gas-liquid levels are frequently present in the lumen of the small bowel, indicating the presence of dynamical abnormalities. Bowel wall thickening and transmural inflammatory changes, such as mesenteric fat deposition, increased vasculature and fibrotic peritoneal thickening, were usually particularly striking in the adhered bowel segments. A segment of adhesive bowel loop

with peritoneal involvement forms the so-called "abdominal cocoon"[29-32]. In this study, various abdominal cocoons, such as the "accordion sign", "cauliflower sign" and "bottle gourd sign", were found. An adhesive bowel loop was present in 15 patients [cases 1 (Figure 14), 2 (Figure 12), 3 (Figure 3), 4 (Figure 1), 6 (Figure 4), 7 (Figure 15), 8 (Figure 16), 9 (Figure 5), 11 (Figure 11), 12 (Figure 7), 13 (Figure 2), 14 (Figure 8), 15 (Figure 10), 16 (Figure 17), and 17 (Figure 13)]. The high incidence of an adhesive bowel loop suggested the presence of high prevalence of chronic active bowel inflammatory damage in the small intestine in patients with SAA. In the 2 patients without an adhesive bowel loop, cases 5 (Figure 9) and 10 (Figure 6) presented with striking hypervascular mesenteric fat proliferation and a widened bowel loop (creeping fat sign), also indicating the presence of active chronic inflammatory involvement of the small intestine[24-26]. Although these inflammatory lesions in the small bowel might not serve as the major factors in the regulation of hematopoietic and immune functions, they exert an important role that affects the downstream gut microbial community and thereby affects downstream intestinal barrier function[54-56].

The ileocecal region is the most common site for various infectious and inflammatory diseases[9,10,14,16]. In this study, all patients with SAA presented with inflammatory involvement of the ileoceal region. Among them, 2 patients presented with inflammatory lesions in the ileocecal region as the predominant imaging presentation. In case 1 (Figure 14), the prominent inflammatory lesion was a large omentum-encapsulated inflammatory mass centered on the homogeneously wall-thickened appendix and extending to the scrotum along the inguinal canal. In case 7 (Figure 15), the particularly prominent inflammatory lesion was a cluster of misty fat stranding wrapping the thickened and strictured distal ileum.

Concomitant extraabdominal presentations may confer useful information for a suggestive etiopathological diagnosis. In this study, pleural involvement of hypertrophic lesions was present in 4 patients [cases 5 (Figure 10), 8 (Figure 16), 16 (Figure 17) and 17 (Figure 13)], strongly suggestive of tuberculosis infection. However, no tuberculotic lesions were present in their lungs. In addition to the pleural

involvement, 1 patients [case 13 (Figure 2)] presented with peritoneal involvement of hypertrophic lesions, also suggesting the presence of tuberculosis infection.

Taken together, this radiological study demonstrated the gut involvement of various inflammatory changes in all patients with SAA. The inflammatory lesions concurrently affected the large intestine, ileocaecal region and small intestine. Although compromised intestinal integrity in the ileocecal region and large intestine exerts a major role in the development of hematological and immunological diseases[9-13], inflammatory damage and dysfunction in the upper gastrointestinal tract can affect the pathophysiologies of the downstream intestinal integrity[54-56] and thereby exert an indirect impact on hematological and immunological function. In susceptible individuals, active chronic gut inflammatory conditions may initiate and perpetuate hematological damage, and aggravated gut damages may induce flared episodes[4-8].

During flared episodes, the imaging features suggested the presence of chronic gut inflammatory conditions and acutely aggravated inflammatory damages. Some readily recognized imaging signs, such as bowel wall thickening with mural stratification ("water holo sign", "fat holo sign", intramural gas and subserosal pneumatoses) and mesenteric fat proliferation (fat stranding and "creeping fat sign"), "balloon sign", rugged colonic configuration and adhesive bowel loop (including various patterns of abdominal cocoon), occurred at a high incidence, which suggested that the gastrointestinal tract is common inflammatory niche responsible for the systemic inflammatory stresses in patients with SAA. Successful treatment of their gut inflammatory conditions significantly improves their hematological profile[4-6], providing convincing evidence for a role of gut inflammation in hematopoietic suppression.

Although not able to provide an etiopathological diagnosis, abdominal CT can provide useful information for exploring gut inflammatory conditions and guiding further work-ups. In this study, a suggestive diagnosis of Crohn's disease was made in 5 patients, ulcerative colitis in 1 patient, chronic periappendiceal abscess in 1 patient, and tuberculosis infection in 5 patients[57-59]. Although the presence of abdominal

cocoons has been reported to have a high probability of tuberculosis infection[31,32] and there was a high incidence of abdominal cocoons present in this study, it was difficult to make a presumptive diagnosis of tuberculosis infection in patients with abdominal cocoons other than the abovementioned 5 patients.

This study had several limitations. First, although CT has some advantages in the detection of the site, extent, degree and peripheral changes of gut inflammatory damage, the exact pathogenic factors cannot be identified, and arriving at an etiopathological diagnosis frequently requires other laboratory tests. This study lacked the endoscopic, pathological and other definitive diagnostic examinations largely due to the contraindication of operative procedures resulting from the very low platelet count and the platelet transfusion refractoriness of these patients. Second, the number of studied patients was quite small, leading to the incidence of each imaging sign being less representative of the actual incidence. Third, the treatment responses by suggested radiological diagnosis were not summarized.

CONCLUSION

All patients with SAA during inflammatory episodes demonstrated gut involvement of both active chronic inflammatory conditions and acute inflammatory damage, providing further evidence to demonstrate the role of GIDs in the pathogenesis of immune-mediated hematopoietic failure. Although arriving at an etiopathological diagnosis frequently requires other laboratory tests, abdominal CT imaging can provide highly useful information for the exploration of gut inflammatory damage and is very helpful for the suggestion of an effective treatment modality. In patients with aggravated cytopenia and clinical presentations suggestive of the presence of inflammatory responses, inflammatory diseases in the gastrointestinal tract should be considered, abdominal CT should be performed, and imaging signs that suggest the presence of gut inflammatory lesions should be carefully identified.

ARTICLE HIGHLIGHTS

Research background

The gastrointestinal tract hosts the body's most enriched lymphoid tissues and microbial community and therefore can provide sufficient activated immune cells and continuous intestine-derived antigens to influence the host hematopoietic and immune functions. The gastrointestinal tract is the most common site for infectious and inflammatory diseases. Morphological changes in computed tomography (CT) images can provide useful information that reflects the distribution, extent, and severity of the bowel inflammation and even suggests a pathogenic diagnosis.

Research motivation

Initiation and perpetuation of aplastic anemia (AA) pathogenesis has been found to be associated with gut inflammatory disorders (GIDs). GIDs have a powerful impact on hematopoietic and immune functions. Treatment of GIDs can improve hematological profile and immunological derangement.

Research objectives

To explore CT imaging presentations of gut inflammatory damage in adult patients with severe AA (SAA) and to provoke awareness of GIDs in the pathogenesis of hematological and autoimmune disorders.

Research methods

We retrospectively evaluated the abdominal CT imaging presentations of 17 hospitalized adult patients with SAA in search of the inflammatory niche when they presented with systemic inflammatory stress and exacerbated hematopoietic function.

Research results

All eligible patients with SAA had CT imaging abnormalities that suggested the presence of an impaired intestinal barrier and increased epithelial permeability. The

inflammatory damages were concurrently present in the small intestine, the ileocecal region and the large intestines.

Research conclusions

All patients with SAA had CT imaging patterns that suggested the presence of active chronic inflammatory conditions and aggravated inflammatory damage during flared inflammatory episodes. In patients with aggravated cytopenia and clinical presentations suggestive of the presence of inflammatory responses, inflammatory diseases in the gastrointestinal tract should be considered, abdominal CT should be performed, and imaging signs that suggest the presence of gut inflammatory lesions should be carefully identified.

Research perspectives

Abdominal CT imaging presentations in association with hematopoietic failure and autoimmune diseases warrant extensive investigations.

igure 1 Characteristic images of case 4. The ileocecal valve (yellow arrows), the proximal ascending colon (orange arrows) and the terminal ileum (purple arrows) were significantly thickened and stratified by submucosal fat deposition, forming the so-called "fat holo sign". The irregular contour and the fibrotic thickening of the mucosal folds made the colonic configuration rugged. The mucosa of the cecum and the appendiceal root was fibrously thickened (green arrows), and the appendix was gas-filled. Thickened omentum surrounded the ileocecal region and the ascending colon. From the distal ascending colon to the sigmoid colon (red arrows), the wall was thickened and stratified by edematous submucosal tissues, forming the so-called "water holo sign". In some segments, the colon was emptied. Paracolonic fat stranding was present from the cecum to the sigmoid colon. The disproportionately less severe paracolonic fat stranding suggested that the edematous colon most likely occurred

during an acute episode. The small intestine was heterogeneous in bowel wall texture, and gas-filled in some segments and liquid-filled in other segments, and adhesive bowel loop was found in two segments: One in the middle jejunum (blue arrows) and another in the proximal ileum (a white arrow). The mucosa of the proximal ileum in the adhered bowel loop was fibrotically thickened, with mesenteric fat deposition and adjacent peritoneal thickening forming the so-called "abdominal cocoon".

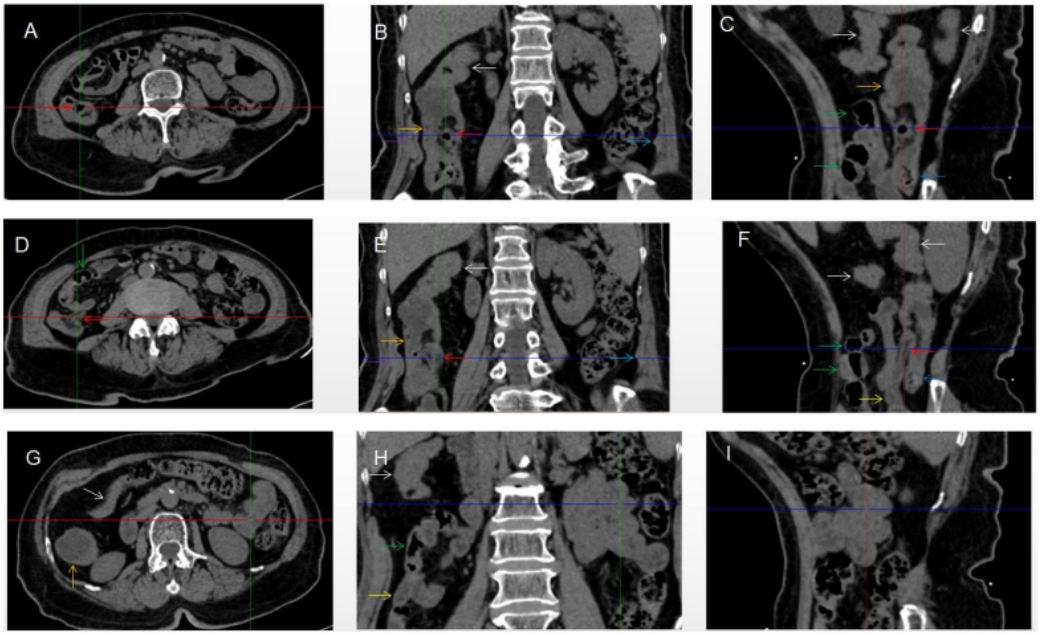

Figure 2 Characteristic images of case 13.

A-C:

D-F:

G-I:

Strictured thickening of the ileocecal valve and terminal ileum (red arrows) led to the distal ileum being liquid-filled, and there was edematous fat deposition around the ileocecal valve and the terminal ileum, forming the so-called "fat holo sign". A massive necrotic lesion in the colonic wall was adjacent to the edematous fat deposition, and the serosal colonic wall was hypertrophically thickened (orange arrows). The adjacent parietal peritoneum (purple arrows) and the left parietal peritoneum (navy blue

arrows) were hypertrophically thickened. The mucosa of the cecum was fibrotically thickened (blue arrow). Edematously thickened colonic wall and emptied colonic lumen were present from the proximal ascending colon to the hepatic flexure, followed by a segment of the collapsed transverse colon (white arrows), forming the so-called "empty colon sign". Proximal to the liquid-filled distal ileum (yellow arrows) was the asymmetrically wall-thickened and gas-filled ileum (green arrows). Heterogeneity of the small bowel wall was observed. A segment of adhesive bowel loop was present in the middle jejunum, together with the fibrotically thickened bowel and peritoneal involvement forming the so-called "cauliflower sign".

Figure 3 Characteristic images of case 3.

A-C:

D-F:

G-I:

The segmentally thickened, stratified (water holo sign) and emptied colon with paracolonic fat stranding was present in the hepatic flexure (yellow arrows) in which an inflamed polypoid lesion was found on endoscopic examination, followed by the asymmetrically thickened wall and gas-filled lumen of the transverse colon (red arrows) in which the colonic villi were absent. The wall of the descending and sigmoid colon was thickened and stratified with mesenteric fat stranding (orange arrows). While the ileum was gas-filled and distended (green arrows), the adhesive jejunal loop (white arrows) was heterogeneous in bowel wall texture and liquid-filled with multiple gas-liquid levels and accrescent plica. Increased mesenteric fat and vascularity were adjacent to the adhered jejunal loop. Clustering and hypervascular mesenteric fat proliferation wrapped a segment of paper-thin ileum, forming the so-called "balloon sign". Balloon sign was also present in the hepatic flexure.

Figure 4 Characteristic images of case 6.

A:

B:

C:

D:

E:

F:

Stratified thickening of the ileocecal valve and the terminal ileum was gas-filled (yellow arrows). Three segments of adhesive jejunal loop were found: one in the distal jejunum (a green arrow); another in the middle jejunum (a purple arrow) in which the bowel wall was asymmetrically thickened and the lumen was gas-filled with particularly prominent mesenteric fat stranding; and the third in the proximal jejunum (white arrows). In the duodenum-jejunum junction (a blue arrow), the bowel wall was fibrotically thickened and the lumen was gas-filled. In the bulb part of the duodenum, a polypoid mass (a black arrow) protruded into the lumen. The wall from the cecum to the descending colon was significantly thickened with mural stratification, intramural gas and pericolonic fat stranding. Several inflamed diverticula (orange arrows) presented in the colonic segments. The sigmoid colon was dilated and the wall was paper-thin (navy blue arrows), with clustering pericolonic fat stranding forming the so-called "balloon sign".

Figure 5 Characteristic images of case 9.

A-C:

D-F:

G-I:

J-L:

The segmentally wall-thickened, stratified and emptied colon in the hepatic flexure (purple arrows) followed by the collapsed transverse (adjacent to the dilated ileum in which gas-liquid levels could be recognized) and descending colon (orange arrows), forming the so-called "empty colon sign". The wall of the ascending colon was thickened and, in some segments, stratified with submucosal fat deposition, and in

other segments, stratified with submucosal edematous tissue (yellow arrows). Several inflamed diverticula (green arrows) were present in the cecum and ascending colon. The ileocecal valve and the terminal ileum were also thickened and stratified by submucosal fat deposition (red arrows). Omental thickening was especially prominent in the ileocecal region. The distal ileum was strictured (blue arrows), proximal to which the ileal lumen was liquid-filled. A short segment of asymmetrically thickened wall was present in the proximal ileum (a white arrow), around which the hypervascular fat stranding was especially prominent, distal to which the ileal lumen was gas-filled, and proximal to which the ileal lumen was liquid-filled. Three segments of liquid-filled adhesive bowel loop were visualized: one in the jejunum and the other two in the proximal and distal ileum. The fibrotic mucosa and liquid-filled lumen of the adhesive bowel loops in the proximal ileum (powder blue arrows) and distal ileum (jade-green arrows), together with the fibrotically thickened peritoneum, formed the so-called abdominal cocoon. A large cluster of circumferentially distributed hypervascular fat stranding wrapped a segment of the dilated lumen and paper-thin bowel wall of the sigmoid colon, forming the so-called “balloon sign”. Hypertrophic lesions presented in two segments of the esophagus (5F), together with the inflammatory lesions in the jejunum suggesting that the initiating factor in the upper gastrointestinal tract affected the functions of the downstream intestinal segments.

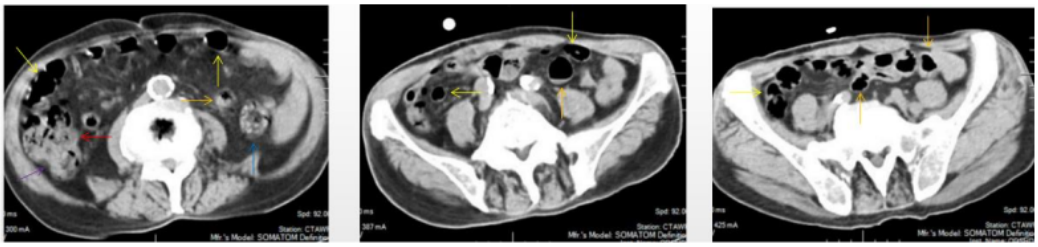

Figure 6 Characteristic images of case 10.

A:

B:

C:

D:

E:

F:

The ileocecal valve and the terminal ileum were significantly thickened, stratified and strictured (red arrows), and proximal to the thickened terminal ileum, the ileal lumen was dilated and gas-filled and the mucosa was hyperdense (yellow arrows). While the proximal ileum and the distal jejunum (orange arrows) were thickened and gas-filled, the duodenum and the proximal jejunum were liquid-filled. The ascending colonic wall was also thickened (purple arrows). In a short segment of the descending colon (blue arrows), accrescent villi were especially prominent. The most noticeable radiological finding was the panabdominal silt-like hypervascular fat deposition, leading to the widening of the bowel loop of the jejunum and the proximal ileum, forming the so-called “creeping fat sign”.

Figure 7 Characteristic images of case 12.

A:

B:

C:

D:

E:

F:

The ileocecal valve and the terminal ileal wall (red arrows) were thickened, stratified and strictured. Proximal to the strictured terminal ileum, the ileal lumen was dilated and gas-filled, and the mucosa was hyperdense. A large cluster of hypervasular mesenteric fat proliferation wrapped the dilated and gas-filled ileum. The jejunum was liquid-filled and the jejunual loop was adhesive. A cluster of hypervascular fat stranding wrapped a short segment of the jejunum (blue arrows), suggesting that the transmural inflammation was more serious in this jejunal segment. The colonic wall was also thickened and stratified, with intramural gas and subserosal pneumatosis (yellow arrows). Mild liquid collection in the pelvic cavity (a green arrow) and the thickened peritoneum (a purple arrow) suggested peritoneal involvement.

The ileocecal valve and the ileal wall were fibrotically thickened and the ileal lumen was gas-filled (yellow arrows), with a large cluster of hypervascular perienteric fat proliferation wrapping the wall-thickened and lumen-dilated ileum. The cecum (blue arrows) and appendix (green arrows) were also fibrotically thickened and stratified, with peripheral fat stranding. Gas-liquid levels were present in the lumen of the proximal ileum and distal jejunum (purple arrows). However, the adhesive jejunal loop was liquid-filled with prominent hypervascular mesenteric fat proliferation. In a segment of the jejunum (white arrows), the bowel wall was thickened, the lumen was gas-filled and the mesenteric fat stranding was especially prominent. Thickened peritoneum was adjacent to the adhesive jejunal loop, forming the so-call “abdominal cocoon” and the enlarged mesenteric vascularity formed the so-called “comb sign”. The

ascending colon was dilated with a paper-thin bowel wall (black arrows), forming the so-called "balloon sign". From the hepatic flexure to the distal descending colon (red arrows), the bowel was thickened and stratified (water holo sign), with paracolonic fat stranding and peritoneal thickening being particular prominent in the hepatic flexure. The sigmoid colon was fibrotically thickened and dilated (orange arrows).

From the cecum to the descending colon, the lumen was dilated, the mucosa was hyperdence and the wall was thickened and stratified in some segments (orange arrows), with striking mesenteric fat stranding. There was a hypertrophic lesion (a red arrow) in the terminal descending colon. The mucosa of the proximal sigmoid colon was hyperdense and the lumen was gas-filled (blue arrows), following which was a short segment of strictured sigmoid colon (yellow arrows). The ileocecal valve and the terminal ileum were thickened and strictured but without mural stratification (a purple arrow), proximal to which the small intestine was liquid-filled. In the ileocecal region, the colonic wall was thickened with smudgy peritoneal thickening (white arrows). Mild ascites presented in both the right and left iliac fossa (green arrows), together with a thickened peritoneum indicative of peritoneal involvement. Chest CT showed the presence of pleural effusion in the bilateral cavities and bilateral pleural hypertrophic thickening. Enlarged blood vessels extended to the hypertrophic lesions.

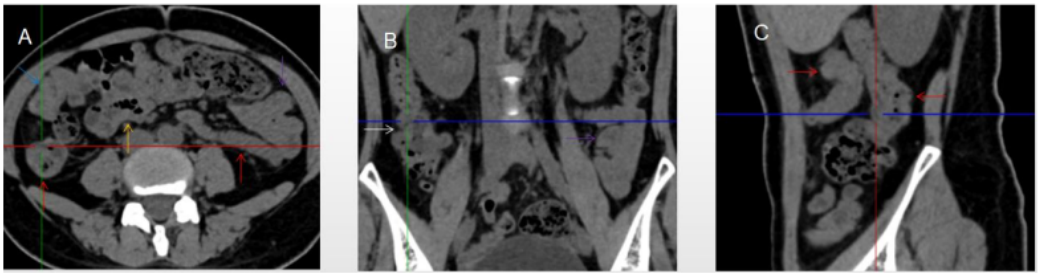

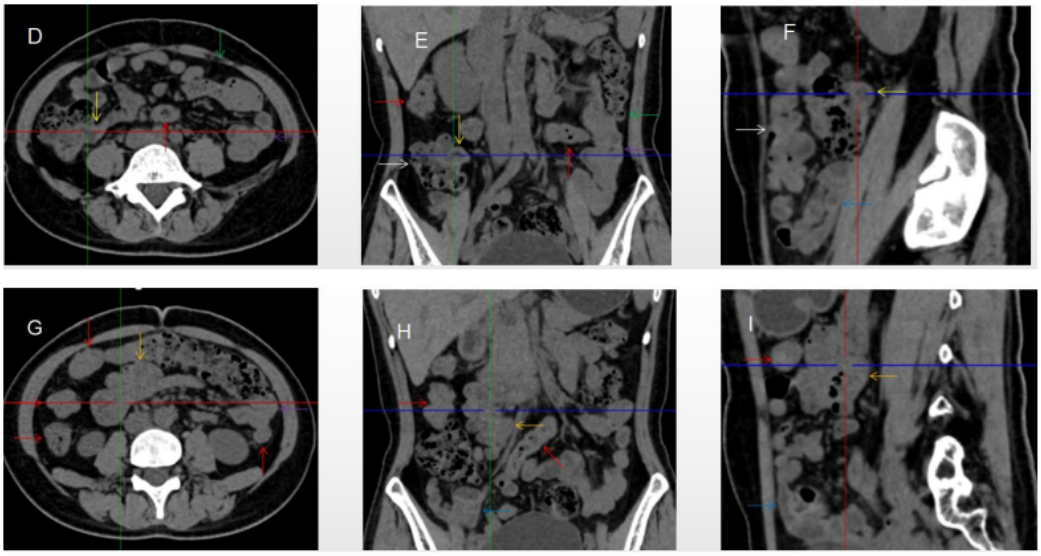

Figure 10 Characteristic images of case 15.

A-C:

D-F:

G-I:

The ileocecal valve and the terminal ileal wall were fibrotically thickened (yellow arrows), proximal to which the ileal lumen was liquid-filled. The ascending colon was rugged with omental thickening and paracolonic fat stranding, and the colonic wall was thickened with mural stratification and intramural gas (white arrows). From the hepatic flexure to the sigmoid colon (red arrows), the bowel wall was thickened and stratified with several inflamed diverticula (green arrows) in the colonic segments. A segment of adhesive bowel loop with liquid-filled lumen and fibrotically thickened bowel wall and peritoneum was present in the distal ileum (blue arrows), forming the so-called "abdominal cocoon". the other two segments of adhesive bowel loops were found in the middle ileum (orange arrows) and the jejunum (purple arrows).

Figure 11 Characteristic images in case 11.

The ascending colon was rugged with fibrotically and irregularly thickened colonic mucosa, circumferentially distributed omental thickening and paracolonic fat stranding (yellow arrows), and other colonic segments were thickened and stratified with water holo sign (red arrows). Several inflamed diverticula was present in the colonic segments (white arrows). The ileocecal valve and the terminal ileal wall were strikingly thickened and stratified (orange arrows). Bowel wall thickening, mural stratification, heterogeneity in bowel wall texture, gas-liquid levels (purple arrows) and adhesive bowel loops were found in the small intestines. In the middle jejunum (blue arrows), a segment of adhesive bowel loop with the peritoneal involvement formed the so-called "cauliflower sign".

Figure 12 Characteristic images of case 2.

A-C:

D-F:

In the ascending and transverse colon (green arrows), the wall was thickened and stratified with "water holo sign", the mucosa was hyperdense and the configuration was rugged, with paracolonic fat stranding, omental thickening and subserosal pneumatoses. The wall of the descending and sigmoid colon (red arrows) was also thickened and stratified, with a particularly striking edematous segment in the rectum. The ileocecal valve and the terminal ileal wall were thickened and stratified (white arrows), the ileal mucosa was hyperdense and the ileal lumen was liquid-filled. In two segments of the adhesive bowel loop (blue arrows and yellow arrows), the bowel wall was heterogeneously thickened and the lumen was gas-filled, suggesting the presence of heterogeneity in small bowel wall texture.

Figure 13 Characteristic images in case 17.

A-C:

D-F:

G-I:

J-L:

M-O:

Circumferentially distributed fat deposition wrapped the ileocecal valve (yellow arrows), forming the so-called “fat holo sign”. The terminal ileum was thickened, and the strictured ileocecal valve and terminal ileum led to the small intestines being liquid-filled. Heterogeneity and hypertrophic lesions of the small intestines were easily recognized. A long segment of the adhered jejunal loop presented in the left iliac fossa and pelvic cavity (green arrows). In the adhesive jejunal loop, the lumen was gas-filled in the proximal segment and liquid-filled in the distal segment. Hypervascular mesenteric fat stranding and fibrotic peritoneal thickening were present in this bowel segment, forming the so-called “abdominal cocoon”. Fibrotic wall thickening was present in the entire jejunal segment and accrescent pili were visualized in the adhesive jejunal loop and the proximal jejunum. Erosive lesions on the background of the calcified lesions were found in the esophagus (13C) and stomach (13D). The ascending colon was rugged with paracolonic fat stranding and peritoneal thickening, and the colonic wall was thickened and stratified with edematous submucosal tissue and intramural gas (orange arrows). From the transverse to the sigmoid colon (red arrows), the colonic wall was fibrotically thickened, with multiple inflamed diverticula in this colonic segment. Hypertrophic lesions and seromembranous effusion were visualized in the pericardium (black arrows) and the pleura (light blue arrows). Exudative lesions were also present in the urinary tract (a purple arrow in Figure 13D) and the vertebral column (blue arrows). These radiological feature led to the diagnosis of reactive tuberculosis infections in the gastrointestinal tract, urinary tract, peritoneum, vertebral column, pleura and pericardium.

Figure 14 Characteristic images of case 1.

A-C:

D-F:

G-I:

J-L:

A massive cluster of fat stranding that was wrapped by the strikingly thickened omentum (purple arrows) was centered on the homogeneously wall-thickened and gas-filled appendix (orange arrows), leading to the diagnosis of a chronic periappendiceal abscess. The periappendiceal inflammatory changes extended to the scrotum along the inguinal canal (red arrows). In the adjacent sigmoid colon, the wall was thickened and stratified with the water holo sign, and the lumen was gas-filled (blue arrows). The ileocecal valve was thickened and strictured (green arrows), proximal to which the ileal lumen was liquid-filled. Bowel wall thickening with irregular mucosal folds, emptied lumen, mural stratification (fat holo sign) and paracolonic fat stranding that was disproportionately less severe then the severity of the colonic wall thickening was present from the cecum to the transverse colon (yellow arrows), suggesting the involvement of a transmural inflammatory condition. In the descending colon, the wall was also fibrotically thickened. A segment of adhesive bowel loop with fibrotic bowel wall thickening, peritoneal thickening and hypervascular mesenteric fat stranding was present in the jejunum (white arrows), together with the segmentally gas-filled, segmentally liquid-filled jejunal lumen, suggesting the inflammatory involvement of the upper gastrointestinal tract.

Figure 15 Characteristic images of case 7.

A:

B:

C:

D:

E:

F:

G-I:

The ileocecal valve was thickened and stratified (yellow arrow). The distal ileum was thickened and strictured (green arrows) with a large cluster of misty exudative lesions surrounding the cecum and distal ileum, and the proximal small intestine was liquid-

filled with multiple gas-liquid levels. From the cecum to the distal descending colon, the mucosa and the villi were hyperdense, with several focally wall-thickened and stratified colonic segments (red arrows) and several inflamed diverticula (blue arrows). An obstructively thickened segment of the sigmoid colon (orange arrows) with prominent paracolonic hypervascular fat stranding was distal to the remarkably distended lumen and paper-thin bowel wall of the sigmoid colon (white arrows).

Figure 16 Characteristic images in case 8.

A-C:

D-F:

G-I:

The ileocecal valve (red arrows) was thickened, strictured and stratified. The distal ileum (yellow arrows) were significantly thickened with intramural gas and wrapped by prominent mesenteric fat stranding, which suggested the presence of aggravated inflammatory damage in the distal ileum and ileocecal region. In the ileocecal region, the ileum adhered to the cecum, and the cecum was thickened and stratified. In other colonic segments (orange arrows), the bowel wall was also thickened and stratified, and the lumen was dilated in some segments and collapsed in other segments. From the jejunum to the proximal ileum (green arrows), the wall was fibrotic and thickened and the lumen was gas-filled. Several segments of adhesive bowel loop were present in the small bowel. Noticeably, panabdominal silt-like hypervascular fat deposition wrapped the adhesive and widened small bowel loop (creeping fat sign), which suggested the presence of chronic transmural inflammatory damage and a diagnosis of Crohn's disease. Chest CT showed exudative lesions in the left pleura in the context of calcified lesions, indicating the reactivation of an old tuberculosis infection.

Figure 17 Characteristic images in case 16.

A-C:

D-F:

The ileocecal valve was fibrotic and thickened with edematous fat deposition, forming the so-called “fat holo sign” (orange arrows), and the distal ileum was adhesive with mesenteric fat stranding and peritoneal thickening (white arrow), forming the so-called “abdominal cocoon”. Intestinal adhesion with bowel wall thickening, peritoneal involvement and mesenteric fat stranding was also found in the jejunum (blue arrow). Heterogeneity in the bowel wall texture was particularly prominent in the adhesive bowel segments. The ascending colon was rugged and the colonic wall was thickened and stratified, with adjacent omental thickening (yellow arrows). The transverse, descending and sigmoid colonic wall were significantly thickened and stratified with mucosal hyperdensity and paracolonic fat stranding (red arrows). Chest CT revealed that the pleural effusion was predominantly in the left cavity and hypertrophic lesions involved both the left pleura and the pericardium (green arrows).

Table 1 Clinical characteristics and rediological diagnosis of the studied patients

No.	Sex/age	Hematological diagnosis	Total duration (yr)	SAA duration (yr)	CBC results					Abdominal symptoms	Suggested radiological diagnosis	Extraintestinal abnormalities
					WBC	ANC	Hb	Plts	Rets			
01	M/54	VSAA	23	8	0.66	0.14	44	5	3.17	AP,AT	CAA	
02	M/46	SAA	16	6	1.24	0.55	42	11	6.16	AT	CEC	
03	F/78	VSAA	11	3	0.65	0.17	41	8	1.81	AP, AT	CD	
04	F/38	SAA	17	6	1.62	0.71	45	18	4.18	AP, AT	CEC	
05	M/71	VSAA	14	4	0.57	0.08	42	2	1.92	AT	UC, ATB?	+
06	M/65	SAA	21	8	1.38	0.42	46	13	5.47	AP, AT	CEC	
07	F/52	SAA	11	5	1.48	0.44	53	21	4.62	AT	CEC	
08	M/61	SAA	21	7	1.73	0.77	62	16	2.28	AT	CD, ATB?	+
09	F/55	SAA	9	3	1.17	0.43	48	6	11.75	AT	CEC	
10	M/77	VSAA	8	4	0.42	0.16	40	4	1.78	AT	CD	
11	M/57	SAA	12	2	1.14	0.36	45	14	6.32	AP, AT	CEC	
12	F/48	SAA	12	6	0.92	0.44	40	3	2.08	AT	CD	
13	F/34	SAA	18	7	0.92	0.31	62	7	1.59	AP, AT	ATB?	+
14	F/40	SAA	13	4	0.86	0.27	44	2	6.03	AP, AT	CD	

15	F/42	SAA	20	9	0.82	0.39	51	18	2.14	AT	CEC	
16	M/68	VSAA	10	3	0.47	0.14	39	6	3.44	AT	CEC, ATB?	+
17	F/36	SAA	11	3	1.38	0.31	46	9	8.41	AP, AT	ATB?	+

M: Male; F: Female; SAA: Severe aplastic anemia; VSAA: Very-SAA; WBC: White blood cells (× 10^9/L); CBC: Complete blood cell count; WBC: White blood cell count; ANC: Absolute neutrophil count (× 10^9/L); Hb: Hemoglobulin (g/L); Plt: Platelets (× 10^9/L); Ret: Absolute reticulocyte count (× 10^9/L); AP: Abdominal pain; AT: Abdominal tenderness; CAA: Chronic appendiceal abscess; CEC: Chronic enterocolitis; ATB: Abdominal tuberculosis; CD: Crohn's disease; UC: Ulcerative colitis.

80895_Auto_Edited-check.docx

ORIGINALITY REPORT

6%
SIMILARITY INDEX

PRIMARY SOURCES

1	Abdominal Imaging, 2013. Crossref	147 words — 2%
2	www.science.gov Internet	50 words — 1%
3	"Operative Strategies in Inflammatory Bowel Disease", Springer Science and Business Media LLC, 1999 Crossref	38 words — < 1%
4	deschutescountyor.iqm2.com Internet	38 words — < 1%
5	link.springer.com Internet	37 words — < 1%
6	slideheaven.com Internet	33 words — < 1%
7	Piero Boraschi, Luigi Giugliano, Giuseppe Mercogliano, Francescamaria Donati, Stefania Romano, Emanuele Neri. "Abdominal and gastrointestinal manifestations in COVID-19 patients: Is imaging useful?", World Journal of Gastroenterology, 2021 Crossref	18 words — < 1%

8	Gore, Richard, Daniel Wenzke, Robert Silvers, Geraldine Newmark, Kiran Thakrar, Uday Mehta, and Jonathan Berlin. "Pathology of the Stomach and Small Bowel", Multi-Detector CT Imaging Abdomen Pelvis and CAD Applications, 2013. Crossref	16 words — < 1%
9	Mario Sergio Pergolini. "Posters", Internal and Emergency Medicine, 2012 Crossref	16 words — < 1%
10	core.ac.uk Internet	15 words — < 1%
11	synapse.koreamed.org Internet	14 words — < 1%
12	www.coursehero.com Internet	14 words — < 1%
13	www.dovepress.com Internet	14 words — < 1%
14	pesquisa.bvsalud.org Internet	12 words — < 1%
15	David Gómez-Almaguer. "Subcutaneous alemtuzumab plus cyclosporine for the treatment of aplastic anemia", Annals of Hematology, 08/25/2009 Crossref	11 words — < 1%
16	Lee-Elliott, C.. "Small bowel MRI imaging in the DGH - Are you doing it yet?", Clinical Radiology, 201206 Crossref	10 words — < 1%
17	ddd.uab.cat	

	Internet	10 words — < 1%
18	haematologica.org Internet	10 words — < 1%
19	www.frontiersin.org Internet	10 words — < 1%
20	f6publishing.blob.core.windows.net Internet	9 words — < 1%
21	journals.lww.com Internet	9 words — < 1%
22	www.mdpi.com Internet	9 words — < 1%
23	Terrell E. Jones, Aaron J. Wyse, Sarah E. Gibson. "Hematolymphoid neoplasms are common in bone marrow biopsies performed for non-specific, diffuse marrow signal alterations on magnetic resonance imaging", Annals of Diagnostic Pathology, 2019 Crossref	8 words — < 1%
24	docplayer.net Internet	8 words — < 1%
25	worldwidescience.org Internet	8 words — < 1%
26	A. Radtke. "Territorial belonging of the middle hepatic vein in living liver donor candidates evaluated by three-dimensional computed tomographic reconstruction and virtual liver resection", British Journal of Surgery, 02/2009 Crossref	7 words — < 1%

27 Anke Franzke. BMC Genomics, 2006
Crossref
7 words — < 1%

28 Damian J. M. Tolan, Rebecca Greenhalgh, Ian A. Zealley, Steve Halligan, Stuart A. Taylor. "MR Enterographic Manifestations of Small Bowel Crohn Disease", RadioGraphics, 2010
Crossref
7 words — < 1%

29 Pamela T. Johnson, John Eng, Carolyn J. Moore, Karen M. Horton, Elliot K. Fishman. "Multidetector-row CT of the appendix in healthy adults", Emergency Radiology, 2006
Crossref
7 words — < 1%

EXCLUDE QUOTES	OFF	EXCLUDE SOURCES	OFF
EXCLUDE BIBLIOGRAPHY	OFF	EXCLUDE MATCHES	OFF